

Multibody Dynamics Simulation of a Tiltrotor UAV

Jinwei Shen
Research Scientist

National Institute of Aerospace
Hampton, Virginia, United States

Matt Floros
Aerospace Engineer

U.S. Army Research Laboratory
Hampton, Virginia, United States

Myeong Kyu Lee
Senior Research Engineer

Korea Aerospace Research Institute
Daejeon, Korea

Jai Moo Kim
Principal Research Engineer

Abstract

Rotor performance, controls, and blade loads are compared for a stiff-inplane gimbaled rotor using two analyses. The rotor system of a tilt rotor unmanned aerial vehicle is modeled using the comprehensive analysis CAMRAD II and the multibody dynamics analysis DYMORE II. The models were developed in tandem so that the geometry and other physical characteristics match as closely as possible. Predictions are then compared for vertical ascent with a gust loading, transition between helicopter and airplane flight, and a transient pull-up maneuver. Good correlation is observed between the two models, particularly in 1/rev bending moments for the transient maneuver.

Introduction

The increasing cost of wind-tunnel testing has resulted in increased investment in advanced simulation and modeling for rotorcraft. Systematic use of these analytical models currently supplements and may eventually be an alternative to expensive experimental verifications [1].

Comprehensive, multibody-based analyses of rotorcraft enable the modeling and simulation of the rotor system to a high level of detail such that complex mechanics and nonlinear effects associated with the control system geometry and pylon conversion assembly can be considered. In this paper, a rotor for a proposed tilt-rotor unmanned aerial vehicle (UAV) is examined using the comprehensive analysis CAMRAD II [2] and the multibody dynamics analysis DYMORE [3,4].

Both analyses use a combination of finite element analysis and multibody dynamics principles to account for nonlinear joint motion, large rotations, and other nonlinear phenomena necessary to model the complex kinematics of a modern rotor system. Although the histories, formulations, and model creation and solution procedures of the two analyses are different, models which are substantially the same can be constructed.

To generate a DYMORE model, the user must specify the location, orientation, and connections of every beam, joint, and rigid body to assemble the model from the ground up. This allows a high degree of versatility in what kinds of mechanical systems can be analyzed, but also requires significant effort to build a new model. The process can be partially alleviated by starting with a similar model that already exists and making changes to it rather than building a completely new model. This is typically done for most analyses.

A CAMRAD II model is normally created using the rotorcraft shell provided with the analysis. With the shell, the user can specify the model with very high level inputs, and the complexities of geometry, joints, connections, and assignment of properties are generated automatically in the program core. The user need only modify the core data to add components or make changes that are not available in the shell.

Analytical Model

Detailed analytical models of the tiltrotor UAV have been developed in DYMORE and CAMRAD II. The analyses include dynamic models for parts of the rotor system which historically were not considered in classical rotor analyses, such as hydraulic actuators in the control system, rotating and non-rotating swashplate components, and detailed kinematics of the pitch links, pitch horns, rotor hub, and shaft.

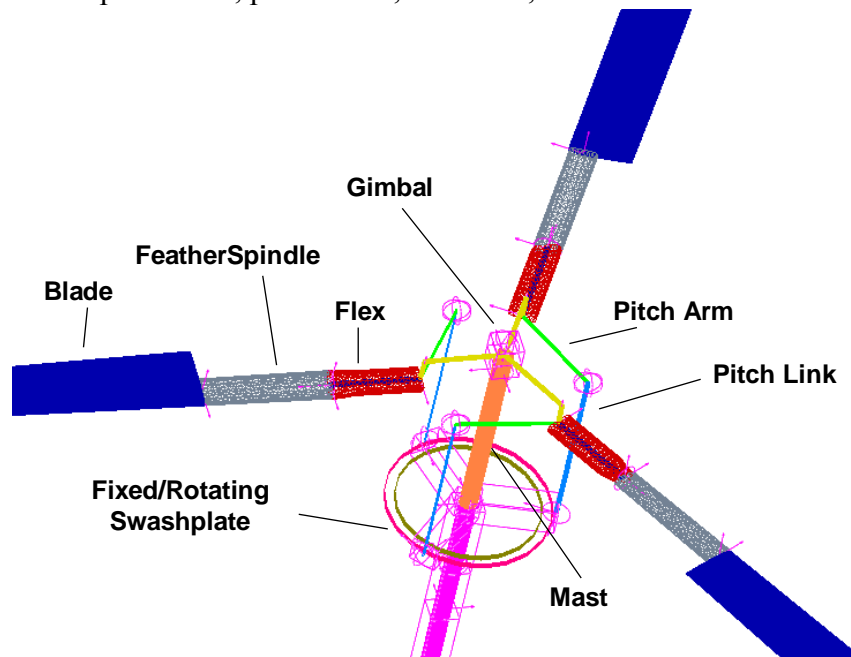


Figure 1 DYMORE model of KARI rotor hub.

In the DYMORE model, the rotor blades are modeled as elastic beams undergoing coupled flap, lag, and torsion deformation similar to the classical rotor analyses. A full-span tilt rotor model was developed for this effort and includes the rotor blades, pitch links, swashplate, pylon, hydraulic control actuators in the pylon, and elastic wings. The pylon conversion actuator is modeled as a flexible joint, which consists of a set of concentrated springs and dampers. The rotor hub, pitch links, pitch horns, swashplate, and pylon are modeled as rigid bodies with appropriate mass and inertia properties. The aerodynamic forces on the rotor are modeled with aerodynamic elements based on lifting line theory. Each blade uses fifteen aerodynamic elements. Rotor inflow is calculated with a three-dimensional nonlinear dynamic inflow model [5]. For this paper, only isolated rotor results are considered, and the wing and pylon degrees of freedom are suppressed. Figure 1 illustrates the key elements of the DYMORE rotor model. The rotor system properties are shown in Table 1.

The CAMRAD II model used in this investigation is an isolated rotor model like the DYMORE II model. The hub, pitch horns, and swashplate are modeled as rigid bodies. Control system stiffness is modeled through the pitch link, which is constructed as a linear joint with a stiff spring. The mass and inertia of the swashplate are considered and couple with the blades in the cyclic rotor modes. The pitch bearing is modeled as a hinge/revolute joint with a small torsion spring to simulate a tension-torsion strap. Also

like the DYMORE model, the aerodynamic model is the uniform inflow option in CAMRAD II, which includes dynamic inflow.

Weight	2000 lb
Max Speed	270 knots
Span (Tip to Tip)	22.3 ft
Fuselage Length	16.4 ft
Rotor Type	Gimbal
Number of Blades (Per Rotor)	3
Rotor Diameter	9.4 ft
Rotor Speed (Cruise)	1284 RPM
Rotor Speed (Hover)	1605 RPM

Table 2 KARI Smart Tiltrotor UAV Properties

Results and Discussion

A detailed set of calculations was specified in support of the UAV design. These loads were intended to identify the critical flight conditions and maximum operational loads the vehicle should encounter in its flight envelope. Load cases examined included hover and vertical ascent, forward flight in helicopter mode, transition to airplane mode, airplane mode flight, and transient maneuvers in airplane mode. Most of the loads cases were steady flight conditions, but some of the load cases were also analyzed in conjunction with a transient vertical gust.

A small selection of the load cases is presented in this paper, including ascending flight with a gust loading, transition to airplane mode, and a transient pull-up maneuver in airplane mode. Control settings, rotor power, and blade loads are compared between the two analyses. In this paper, the blade structural moments are defined as flap bending moments positive tip down, lag bending moments positive tip toward leading edge, and torsion moments positive leading edge up.

Rotor frequency predictions are compared in Table 2. The comparison is carried out at the cruise and helicopter mode rotor speeds, 1284 RPM and 1605 RPM, respectively.

Mode	CAMRAD	DYMORE	CAMRAD	DYMORE
	RPM 1284	RPM 1284	RPM 1605	RPM 1605
Cone	27.57	27.25	32.67	32.37
1 Lag	39.10	37.40	40.12	38.43
2 Flap	82.00	81.67	93.53	93.34
3 Flap	181.19	171.80	195.22	182.57
1 Torsion	222.24	200.08	225.93	206.96

Table 2 Single blade natural frequency (locked gimbal), Hz

Vertical Ascent in Helicopter Mode

The first flight condition to be considered is a vertical ascent at minimum gross weight. When lightly loaded, the vehicle can climb at a speed of nearly 68 knots (6850 ft/min). The flight condition was analyzed both steady state and with a 30 ft/sec vertical gust. The gust profile is a cosine function, referred to as “cosine doublet” in CAMRAD II. For the gust condition, the rotor was analyzed over a 2.5 second interval where the gust is between 1-2 seconds.

Figure 2 compares blade structural moments predicted by CAMRAD II (labeled CII) and DYMORE II (labeled DII). There is good agreement in mean flap bending moments between the CAMRAD II and DYMORE II calculations for both the steady state condition and with the gust. The increase in the mean flap bending moment due to the gust is captured by both analyses. DYMORE calculates loads using a curvature-type method, whereas CAMRAD II uses a force summation-type method. In the root region, there are many structural stiffness changes. The DYMORE loads at some radial stations are calculated from a small curvature multiplied by a large stiffness, which can produce numerical errors. The force summation method is less sensitive to stiffness changes.

Figure 2 (b) and (c) show little change in the mean lag bending moment and torsion moment with the gust. Note that at approximately 0.2R, the CAMRAD II lag bending loads increase sharply while the flap bending loads decrease. This is due to the pitch bearing, where the loads are being rotated through the collective pitch angle and transfer between flap and lag. DYMORE II predicts a larger torsion moment compared to CAMRAD II. Correlation of torsion was generally poor between the two analyses, and the reason is a subject of future investigation.

Figures 2 (d) and (e) show the vibratory half peak-to peak (HPP) moments for the steady state and gust conditions. The vibratory moments in a steady ascent are nearly zero because the rotor is in pure axial flow. The HPP loads are calculated by based on the minimum and maximum moments for the entire time history. Figure 2(d) shows fair agreement between DYMORE and CAMRAD II predictions of vibratory flap bending moments. The lag bending moments appear to show a radial offset between 0.2R and 0.4R where structural properties are changing but at the root flexure, where properties are more uniform, the loads are quite close. The torsion moment, shown in figure 2(f), is quite small, and fair correlation is shown for the two analyses.

Transition Flight

Loads cases were calculated for pylon conversion from 90 degrees (helicopter mode) to 0 deg (airplane mode) at the maximum transition speed. The schedule of pylon angle with forward speed is shown in Figure 3(a). The nacelle angle was held fixed for each calculation. For each nacelle angle, the rotor was trimmed to prescribed thrust and flapping. Loads were calculated from steady state flight at each nacelle angle and steady flight with a vertical gust. Like the vertical ascent, a one-second vertical gust of 30 ft/sec was applied from 1-2 seconds of a 2.5 second record.

For a tilt rotor, a property as simple as collective pitch can be difficult to match because of the large collective range of the rotor. When the rotor is at a large collective pitch setting, the hub kinematics produce a nonlinear relationship between swashplate travel and blade pitch. The collective pitch with airspeed is shown in Figure 3(b). Good agreement is shown between the two analyses, though there is a small offset. Similarly, rotor power, shown in Figure 3(c), agrees well, with slight deviation in the 45-75 degree nacelle region.

Blade loads are shown in Figures 3(d)-(f). In the flap bending loads, there is some deviation in the mid-span region, but the root moments match more closely. The lag moment correlation is not as good, with CAMRAD II predicting a consistently higher lagwise moment than DYMORE II for the 45 and 90 deg nacelle angles. For the 0 deg case, the rotor is in nearly axial flow, producing small oscillatory loads in lag. The torsion moments are quite small for the 0 and 90 deg cases, and differ significantly for 45 deg, where DYMORE II predicts significantly larger oscillatory moments while CAMRAD II does not.

Symmetric Pull-Up Maneuver

The last maneuver considered was a symmetric pull-up maneuver. This maneuver is transient in nature and was modeled by moving the rotor through a prescribed flight path, where vehicle speed, rotor velocities and accelerations (both linear and angular), and collective pitch are specified. The maneuver lasts 10 seconds, with no motion before 1 second and the bulk of the acceleration between 2 and 6 seconds. The maneuver features a large excursion in aircraft pitch, shown in Figure 4(a) along with the collective pitch schedule. There is no yaw or roll motion.

Blade structural moments at 0.4R are shown in Figures 4(b)—(e). The loads were processed with a Fourier transformation, and the mean and 1/rev components of flap and lag bending moments are shown. The mean flapping loads are approximately the same during the steady portions of the maneuver, and there is a 10-15 ft-lb discrepancy in the 2-6 second interval where the angular velocity and acceleration are large. The lag bending moments show a similar trend. Note that the y-axis limits of Figure 4(c) do not contain the origin, so the percentage difference between the two traces is smaller than it appears, about 10% at most.

The 1/rev loads show very good correlation in both flap and lag. Both the magnitude and phase are matched very closely throughout the maneuver. The sine components of the loads increase much more than the cosine components during the maneuver because of the aircraft pitch motion.

Summary

Analytical models of a gimbaled, stiff-inplane tilt rotor for a proposed UAV were developed using CAMRAD II and DYMORE. The two analyses were correlated for control settings, power, and blade loads for steady and transient flight conditions. Flight conditions examined were steady vertical ascent with gust loading, transition flight, and a transient symmetric pull-up maneuver. Rotor controls and power agreed well. Flapping moments generally agreed well with some differences in the inboard region where variable stiffness and geometry complicate loads calculations. Lag moments had fair agreement with CAMRAD II generally predicting larger loads than DYMORE II. Torsion moments were generally small but DYMORE II consistently predicted significantly larger loads than CAMRAD II. For the transient pull-up maneuver, particularly good correlation was observed for 1/rev bending loads.

References

- [1] Nixon, M., Langston, C., Singleton, J., Piatak, D., Kvaternik, R., Corso, L., and Brown, R. "Aeroelastic Stability of a Four-Bladed Semi-Articulated Soft-Inplane Tiltrotor Model,". In *American Helicopter Society 59th Annual Forum Proceedings*, page 11, Phoenix, AZ, May 6-8 2003.
- [2] Johnson, W. "Technology Drivers in the Development of CAMRAD II,". In *American Helicopter Society Aeromechanics Specialists Conference*, San Francisco, CA, January 19-21 1994.
- [3] Bauchau, O., Bottasso, C., and Nikishkov, Y., "Modeling Rotorcraft Dynamics with Finite Element Multibody Procedures," *Mathematical and Computer Modeling*, Vol. 33, :1113–1137, 2001.
- [4] Shen, J., Singleton, J. D., Piatak, D. J., and Bauchau, O. A. "Multibody Dynamics Simulation and Experimental Investigation of a Model-Scale Tiltrotor,". In *American Helicopter Society 61st Annual Forum Proceedings*, Grapevine, TX, June 2005.

- [5] Peters, D. and He, C., "Finite State Induced Flow Models. Part II: Three-Dimensional Rotor Disk," *Journal of Aircraft*, Vol. 32, :323-333, 1995.

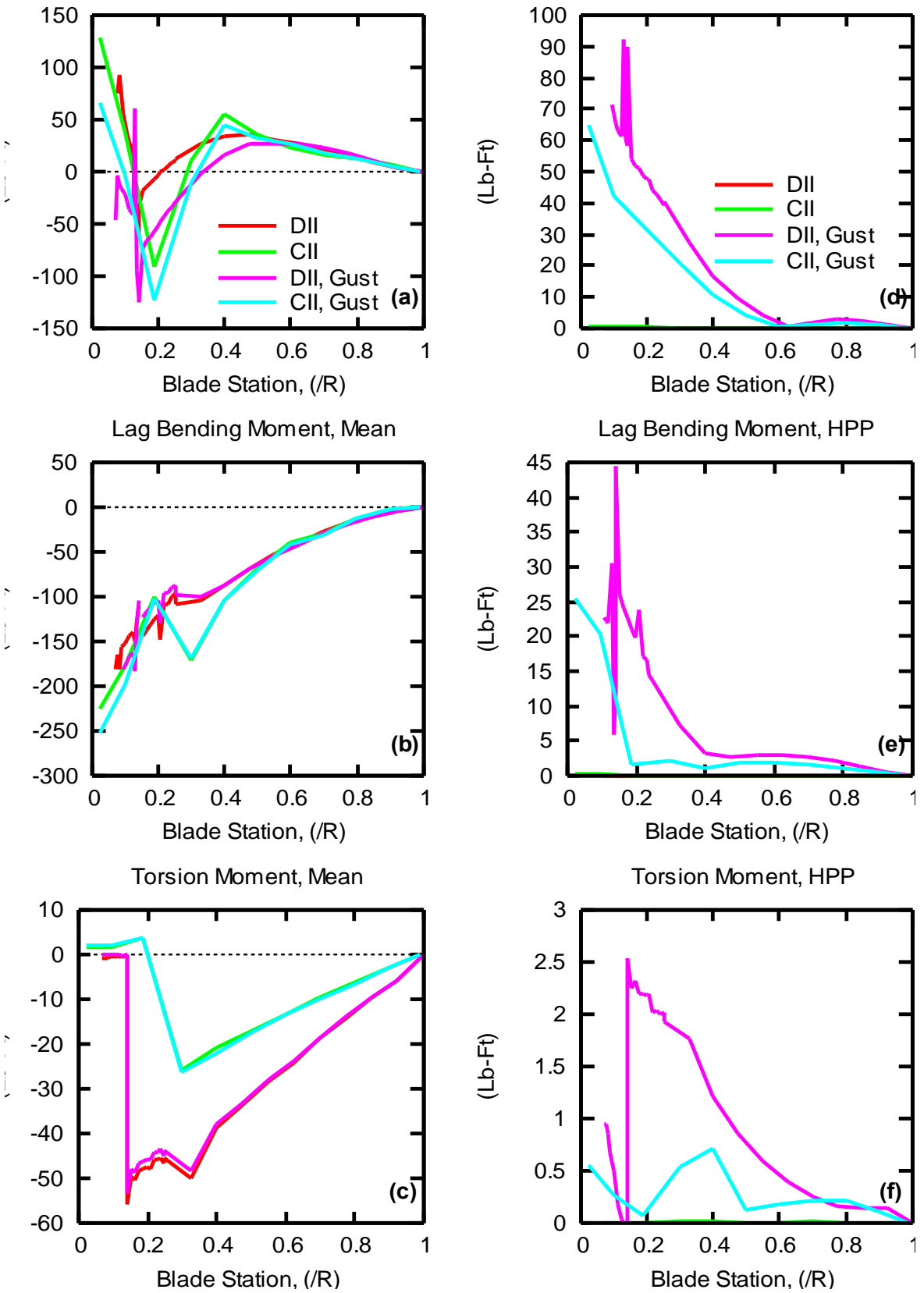


Figure 2 Helicopter mode ascending flight, climbing speed of 68 knots, minimum gross weight of 1614 lb, gust speed of 18 knots.

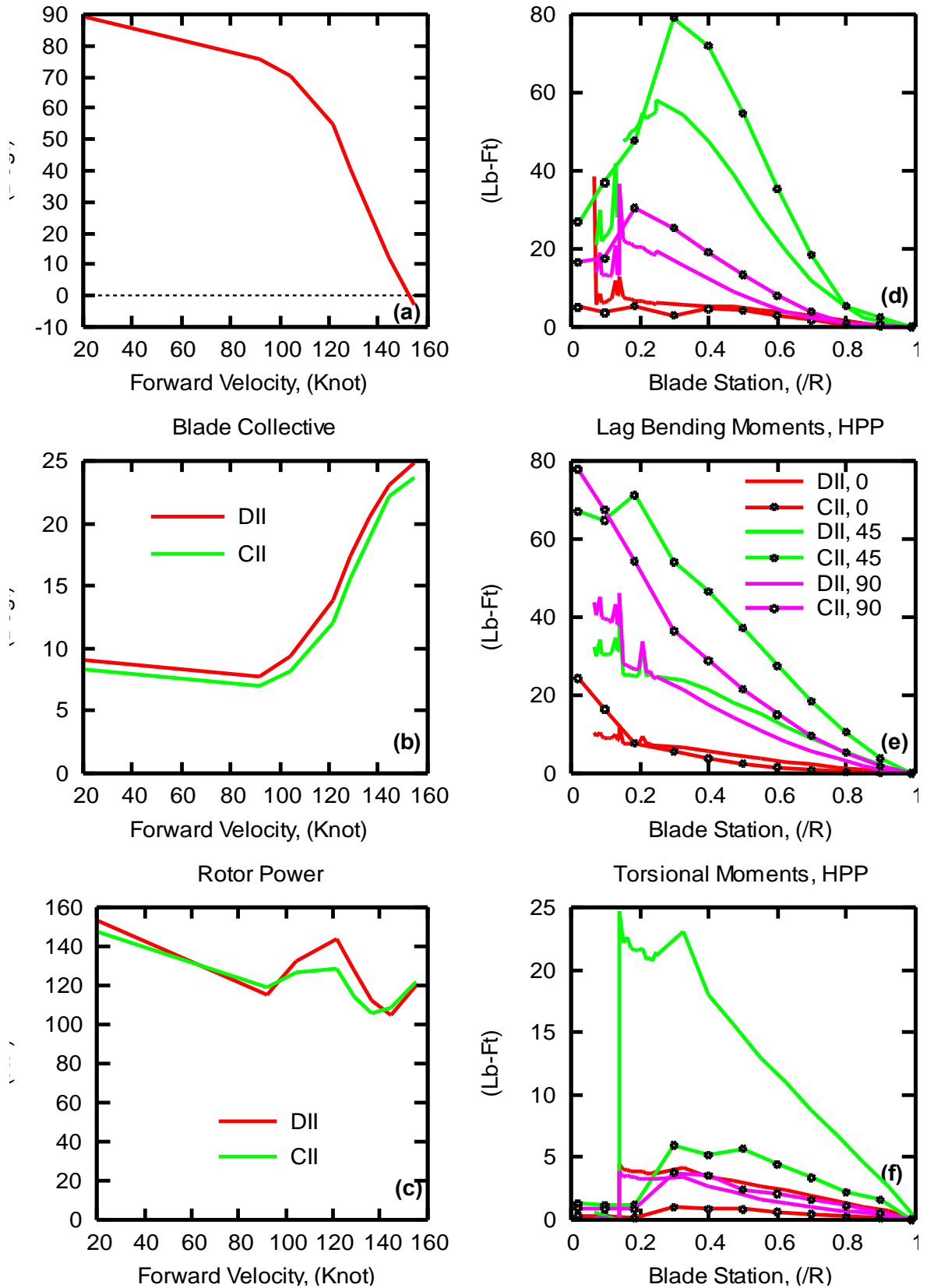


Figure 3 Transition flight at maximum speed, flight condition, collective pitch setting, rotor power, and blade loads at 0, 45, and 90 deg nacelle angle shown.

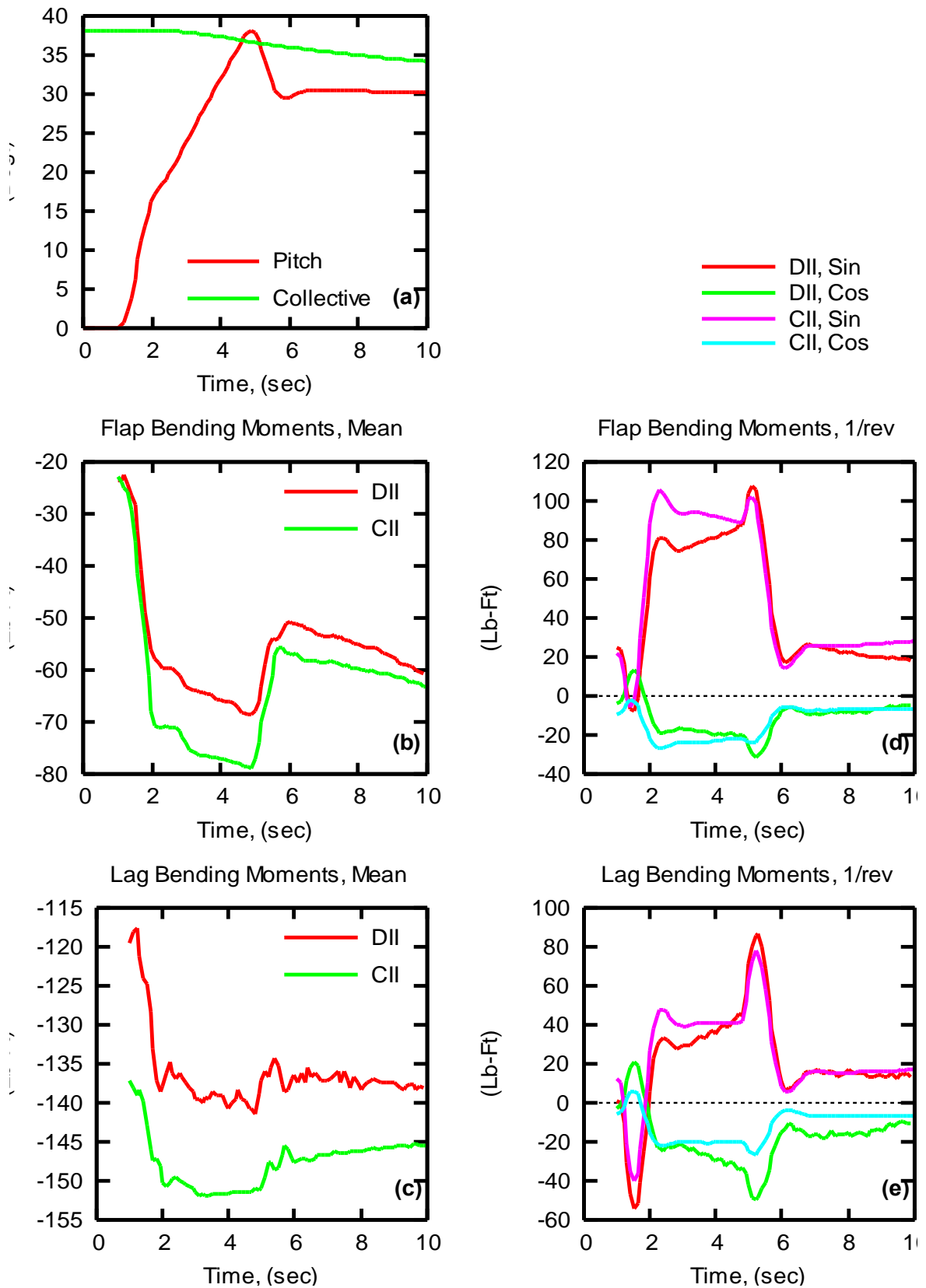


Figure 4 Aircraft pitch, collective pitch setting, and blade loads at 0.4R for symmetric pull-up maneuver.